MAXIMUM ENTROPY PRODUCTION IN BOILING SHOCKS

Oleg Ivashnyov, Marina Ivashneva

Moscow MV Lomonosov State University, Vorobyovi Gori 1, Moscow 119899, Russia

ABSTRACT

Experimental studies of hot water depressurization have shown that liquid boiling proceeds in a shock which moves at a speed of approximately 10 m/s from the open end deep into the tube. The 'boiling shock' was obtained in a numerical experiment using the flow model that considered temperature and velocity non-equilibrium of phases. To analyse the mechanism of an instantaneous evaporation, the wave structure was described with model's stationary version in the moving frame linked with the wave front. From the numerical experiment there were taken all the parameters of nonequilibrium mixture ahead of the wave front but the velocity of the oncoming flow. The velocity was varied to see if a stationary wave-type solution could be obtained. Among the integral curves there was a series of regimes in which the flow velocity went over on a steady level and the mixture reached an equilibrium state. Their analysis showed that an instantaneous transformation of the non-equilibrium boiling mixture into an equilibrium state was caused by a chain bubble fragmentation which led to a sharp increase in the interfacial area, intensification of the vaporization process and loss of liquid's excess heat. Each of stationary wave-type regimes was characterized by a definite meaning of the entropy increase in the shock. It occurred that, in a numerical experiment using a full, non-stationary, system of model equations that was in good agreement with a physical experiment, there realized the regime with a maximum entropy production.

INTRODUCTION

Boiling shocks are formed in flows with accelerations of tens-hundreds metres per second. Such flows are most of interest since they are realized under loss-of-coolant nuclear power stations accidents.

In a classic experiment on a high-pressure vessel depressurization of Edwards and O'Brien [1], the vessel was a 4 m length horizontal tube with 7.3 cm internal diameter. The tube initially contained hot water with temperature 515 K. The pressure in the tube, P_0=6.9 MPa, was twice the pressure of saturation and the water did not boil. The right-hand end of the tube was closed with a glass disc. On destroying the disc, the liquid efflux accompanied by boiling started. A uniform pressure of 2.7 MPa, which was less than the pressure of saturation (3.5 MPa) but greater than an atmospheric one, settled all over the vessel.

In large-scale experimental pressure oscillograms (figure 1), the first waves crossing the channel within 3 ms looked like an instant pressure drop up to P=2.7 MPa at zero time. The pressure remained constant for a long time: only after 0.2 s did it start to decrease rapidly at the 3rd point, and then at the 4th and 5th points. This was the second wave of rarefaction, a 'slow wave', moving with the speed of only 10 m s^{-1}. The experimental oscillograms of the pressure and volumetric vapor fraction measured at the 4th point (solid lines in figure 3*a,b*) showed that the pressure drop in the 'slow wave' was accompanied by the increase in the volumetric vapour content from 0.2 to 0.9.

Slow waves of boiling were observed in Edwards and O'Brien's experiments at different initial parameters of water and in the experiments with the other fluids: CO_2 [2] and dichlorodifluoromethane [3].

HIGH-PRESSURE VESSEL DECOMPRESSION IN THE FRAMES OF AN EQUILIBRIUM MODEL

An equilibrium model [4] includes the equations of conservation for mixture mass, momentum and entropy:

$$\frac{\partial \rho}{\partial t} + \frac{\partial (\rho u)}{\partial x} = 0 , \tag{1}$$

$$\frac{\partial (\rho u)}{\partial t} + \frac{\partial \left(\rho u^2 + P\right)}{\partial x} = 0 , \tag{2}$$

$$\frac{\partial S}{dt} = 0 . \tag{3}$$

The equation of state for an equilibrium mixture is a sectionally continuous dependence between the mixture density, pressure and entropy. It consists of two parts. At the point of their intersection (the point of boiling inception) the derivative of density with respect to pressure breaks:

$$\rho = \begin{cases} \rho_l (P, S_l), & \text{if } P \geq P_S(T_0), \\ \left(\dfrac{1}{\rho_l} + \varphi(P)\left(S - S_l\right) \right)^{-1}, & \text{if } P < P_S(T_0), \end{cases} \tag{4}$$

$$\varphi(P) = \left(\frac{\partial T}{\partial P} \right)_S .$$

The first part of (4) is the equation of state for a pure liquid and the second one is that for an equilibrium mixture.

The isoentropic curve for an equilibrium mixture expansion is shown by a dashed line in figure 3*c*.

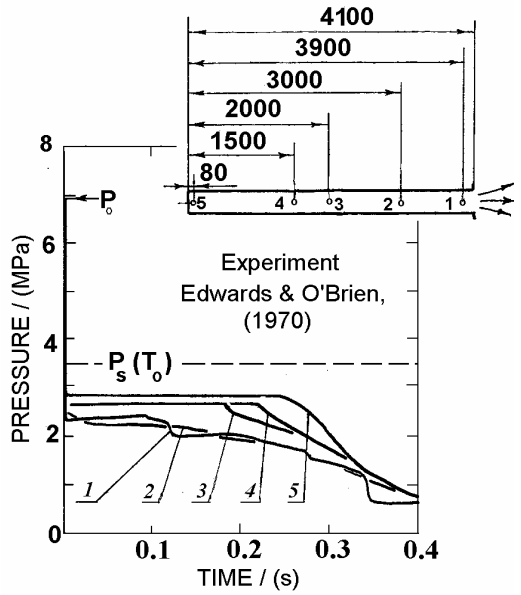

Figure 1. Experimental pressure oscillograms at five different tube cross-section locations (shown in the insert).

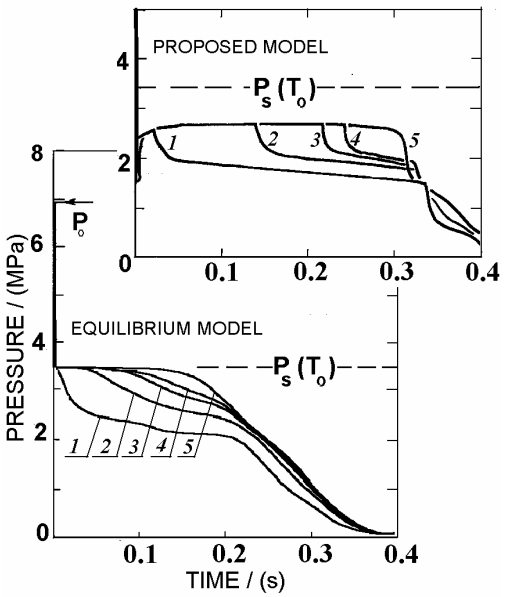

Figure 2. Calculations using an equilibrium and nonequilibrium models of boiling.

It follows from the equation of state (4) that at $P=P_s(T_o)$, the speed of sound

$$a_e = \left(\frac{\partial P}{\partial \rho}\right)_{S=\text{const}}^{-1/2}$$

changes instantaneously from the speed of sound in a pure liquid, 1100 m s^{-1}, down to the speed of sound in an equilibrium two-phase mixture

$$a_e = \left\{\frac{\rho}{\rho_l^2 a_l^2} + \rho\left[\left(1-\frac{\rho}{\rho_l}\right)\frac{1}{\varphi}\left(\frac{\partial^2 T}{\partial P^2}\right)_S - \frac{\rho\varphi}{\rho_l T}\left(\rho_l\left(\frac{\partial i_l}{\partial P}\right)_S - 1\right)\right]\right\}^{-\frac{1}{2}},$$

which is much less, 26 m s^{-1} (at 515 K). Therefore the wave of rarefaction is split into two waves moving with different velocities. The first wave where the pressure drops down to the pressure $P_S(T_0)$ spreads with the speed 1100m s^{-1}. The second wave, where further diminishing of the pressure occurs, moves with the speed of 26 m s^{-1}. These two waves are separated by a zone of constant pressure.

The calculations using the equilibrium model are shown in figure 2 and by dashed lines in figure 3. The two parts of the rarefaction wave are seen (in multi-scale oscillograms, the first one looks like a vertical pressure drop at zero time). According to calculations the pressure behind the first wave of rarefaction is equal to the pressure of saturation, 3.5 MPa, while in the experiment it is much less, 2.7 MPa.

Using experimental oscillograms of pressure and volumetric vapour content the curves of the mixture expansion in P-V (pressure-specific volume) coordinates have been built (figure 3*c*). Their comparison with curves for an adiabatic expansion of an equilibrium mixture have shown that the 1st rarefaction wave converts the mixture into a metastable, overheated, state and the 2nd one turns it back to equilibrium.

DECOMPRESSION IN THE FRAMES OF THE MODEL ACCOUNTING FOR THEMPERATURE AND VELOCITY NON-EQUILIBRIUM OF PHASES

In the model, the boiling is considered to start up at centers of nucleation. The pressures in the phases are assumed to be equal; the parameters in a bubble are uniform and equal to the parameters on the line of saturation; the vapour density is much less that the liquid density; the phase slip is much less than the flow velocity.

Along with the equations (1), (2) for mixture mass and momentum conservation, the model comprises the equations of conservation for internal energy, vapour mass, bubble number, and the equation of motion of an individual bubble:

$$\frac{\partial i}{\partial t} - \frac{1}{\rho}\frac{dP}{dt} = 0, \tag{5}$$

$$\frac{\partial(\rho_g \alpha)}{\partial t} + \frac{\partial(\rho_g \alpha u)}{\partial x} = jn, \tag{6}$$

$$\frac{\partial n}{\partial t} + \frac{\partial(nu)}{\partial x} = \rho\psi, \tag{7}$$

$$\begin{aligned}&\left(\rho_g + C_{vm}\rho_l\right)\frac{d_g u_g}{dt} = \rho_l \frac{Du}{Dt} + C_{vm}\rho_l \frac{Du}{Dt} - \\ &-\frac{3}{a}C_{vm}\rho_l\left(u_g - u\right)\frac{d_g r}{dt} - \left(\frac{3}{2a}C_\mu \rho_l \left|u_g - u\right|\right)\left(u_g - u\right)\end{aligned}, \tag{8}$$

$$\rho = (1-\alpha)\rho_l + \alpha\rho_g,$$

$$i = (1-\chi)i_l + \chi i_g, \quad \chi = \frac{\rho_g \alpha}{\rho}, \tag{9}$$

$$\frac{D}{Dt} = \frac{\partial}{\partial t} + u\frac{\partial}{\partial x}, \quad \frac{d_g}{dt} = \frac{\partial}{\partial t} + u_g\frac{\partial}{\partial x}.$$

Virtual mass coefficient C_{vm} is equal to 1/2 for spherical bubbles. D/Dt is the material derivative following the mixture and d_g/dt is that following the bubbles.

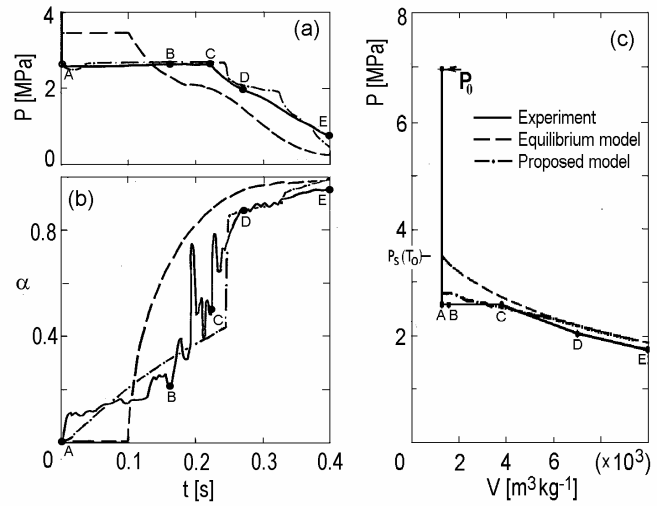

Figure 3. (a,b) A comparison of experimental and theoretical oscillograms of pressure and volumetric vapour content for point 4 (see figure 1). (c) Experimental (built using parameters' values at points ABCDE marked in *a,b*) and theoretical pressure-specific volume dependencies.

Neglecting the dependence of liquid density on temperature, and considering that, nearby the saturation line, the isotherms built in *P-V* coordinates are strait lines, we used the equation of the liquid state in the following form:

$$\frac{1}{\rho_l} = k - \frac{P}{\beta^2},$$
$$\beta = \beta(T_0) = \text{const}, \quad k(T_0) = \frac{1}{\rho_{lS}(T_0)} + \frac{P_S(T_0)}{[\beta(T_0)]^2} = \text{const} \tag{10}$$

Then thermal-energy equation for the liquid state is:

$$i_l(P,T_l) = i_{lS}(T_l) + k\left(P - P_s(T_l)\right) - \frac{P^2 - P_S^2(T_l)}{2\beta^2}, \tag{11}$$
$$i_{lS} = \mathrm{B}(T_l - \mathrm{D})$$

where i_{lS} is the liquid enthalpy on the line of saturation, B=5000 $m^2/(c^2\,K)$, D=305 K are approximation parameters.

Differentiating (11) we obtain specific isobaric thermal capacity of the liquid *h*

$$h = \left(\frac{\partial i_l}{\partial T_l}\right)_P = \mathrm{B} - \frac{1}{\varphi(P_S(T_l))}\left(k - \frac{P_S(T_l)}{\beta^2}\right), \tag{12}$$

where $\varphi(P)$ is the derivative taken along the line of saturation.

For the wide range of temperatures, $450\,\mathrm{K} \le T_S \le 590\,\mathrm{K}$, the approximation $\rho_g = P_g / \mathrm{A}$, $\mathrm{A} = 2\cdot 10^5\ m^2/s^2$ describes the vapour state on the line of saturation with a relative error of 2%.

The intensity of bubble breakup ψ is defined with a relaxation ratio:

$$\psi = \frac{c^* - c}{\tau^*}, \tag{13}$$

where c^* is the number of bubbles that would be formed if the fragmentation were instantaneous, and τ^* is the characteristic fragmentation time which are specified using the solution of the problem about the rise in amplitude of a small harmonic perturbation with wavelength λ arising on a plane interphase boundary [5]:

$$\xi = K \exp\left[I(\lambda)\, t - \mathrm{i}\frac{2\pi}{\lambda} x \right],$$
$$I(\lambda) = \pm\sqrt{\frac{4\pi^2}{\lambda^2}\frac{\rho_g (u_g - u_l)}{\rho_l} - \frac{8\pi^3}{\lambda^3}\frac{\sigma}{\rho_l}}$$

From the condition that a bubble is divided by the wave with the fastest growing amplitude,

$$\lambda^* = \frac{3\pi\sigma}{\rho_g (u_g - u_l)^2},$$

the number of fragments appeared as a result of a bubble breakup (c^*/c) is determined as the ratio of the bubble diameter to the length of the wave λ^*. A characteristic time of breakup is adopted to be the time of e-time (e=2.7...) rise in amplitude of the perturbation with wavelength λ^*. From an evident condition: $\lambda^* \le 2r$, one obtains the criterion of the surface stability of the bubble overflowing by fluid, the Weber number:

$$We = \frac{2\, r\, \rho_g (u_g - u_l)^2}{\sigma}, \tag{14}$$

and the evaluation of its critical value, $We^* = 3\pi$.

$$\frac{c^*}{c} = \frac{2r}{\lambda^*} = \frac{We}{We^*}, \quad \tau^* \sim \sqrt{\frac{\rho_l r^3}{\sigma}\left(\frac{We}{We^*}\right)^3} \tag{15}$$

Δu in the equation (14) is determined from the equation for motion of an individual dispersed unit (8) by:

$$\frac{D}{Dt}\left(\frac{u_g - u}{\rho_g}\right) = \\ = \frac{2}{\rho_g}\frac{Du}{Dt} - \frac{3}{4r}\left[C_\mu \left|u_g - u\right| + \frac{j}{\pi r^2 \rho_g}\right]\frac{u_g - u}{\rho_g} \tag{16}$$

Where D/Dt is the material derivative following the mixture which substitutes the material derivative following the bubbles d_g/dt taking into account the assumption about the smallness of the phase slip, $\left|u_g - u_l\right| << u_l$.

The expression for the interfacial drag coefficient C_μ is:

$$C_\mu = \begin{cases} \dfrac{16}{\mathrm{Re}}, & \mathrm{Re} \le 10.9, \\ \dfrac{48}{\mathrm{Re}}\left(1 - \dfrac{2.2}{\sqrt{\mathrm{Re}}}\right), & 10.9 < \mathrm{Re} \le 1000, \\ 4.466\times 10^{-2}, & \mathrm{Re} > 1000, \end{cases}$$
$$\mathrm{Re} = 2\, r\, \rho_l \frac{\left|u_g - u\right|}{\mu}.$$

Following [6] the intensity of liquid evaporation into a bubble *j* is defined using an automodel solution about a motionless bubble growth in an overheated liquid [7] as:

$$j = \frac{2\pi\gamma}{l} r\, Nu \left[T_l - T_S(P)\right].$$

$$Nu = 2 + \left(\frac{6\,Ja}{\pi}\right)^{1/3} = \frac{12\,Ja}{\pi}, \quad Ja = \frac{h\rho_l (T_l - T_S)}{\rho_g l}$$

From (16), it follows that the liquid acceleration is the only reason of the disturbance of the equality in the phase velocities.

The number of initial bubbles and the critical Weber number are specified as: $c_0 = 4\times10^5$ kg^{-1}, We*=1.

The numerical results obtained using the model (for more details one may see [8]) correspond to experimental ones: the pressure level (2.7 MPa) remains constant for a long time and then suddenly drops (figure 2, upper section); the decrease of pressure is accompanied by the increase in the volumetric vapour content (dashed-dotted lines in figure 3). Thus the shock of boiling has been obtained in the numerical experiment.

THE STRUCTURE OF THE BOILING SHOCK

The width of the 'boiling wave' is small and does not increase in time that allows us to suppose that it can be described by stationary equations in the coordinate system linked with it:

$$G = \rho u = \text{const}, \tag{17}$$

$$Gu + P = \text{const}, \tag{18}$$

$$i + \frac{u^2}{2} = \text{const}, \tag{19}$$

$$\frac{\partial u}{\partial z} = \frac{cj\rho\left(1/\rho_g - 1/\rho_l\right)}{1 - u^2/a_f^2}, \tag{20}$$

$$\frac{d}{dz}\left[\alpha\Delta u\right] = 2\alpha\frac{du}{dz} - \frac{3C_\mu|\Delta u|}{4ru}\left[\alpha\Delta u\right], \tag{21}$$

The frozen speed of sound a_f, the velocity of high-frequency indignations spread in the absence of interphase transfer processes, is determined as:

$$a_f = \left[\rho\left(\frac{(1-\alpha)\rho_l}{\beta^2} + \frac{\alpha}{P}\right)\right]^{-1/2}.$$

All the parameters at z=0 but the velocity of the oncoming flow u* are taken from the numerical experiment given in figure 2 (upper section): P=2.7 MPa, T=513 K, $\alpha = 0.2$ c=c_0=4×10^5 kg^{-1} and We=We*.

Parameters profiles obtained at different u* values are presented in figure 4. At a starting point of the wave, the Weber number reaches its critical value and bubbles begin to break-up. Due to the fragmentation the interfacial area increases and boiling intensifies. The pressure decreases (since the bubble number c is in the numerator of 20). The increase in velocity gradient du/dz causes an increase in the difference of phase velocities Δu (see 21). The increase in Δu is why the Weber number (14) does not decrease after breakup in spite of the diminishing of bubble radius and so breakup is repeated. Thus, it proceeds like a chain reaction, i.e. one breakup creates the conditions for the next one. That leads to the great increase in bubble number. The bubble fragmentation comes to an end when the mixture reaches an equilibrium state ($T_l = T_g$). Then, the intensity of the

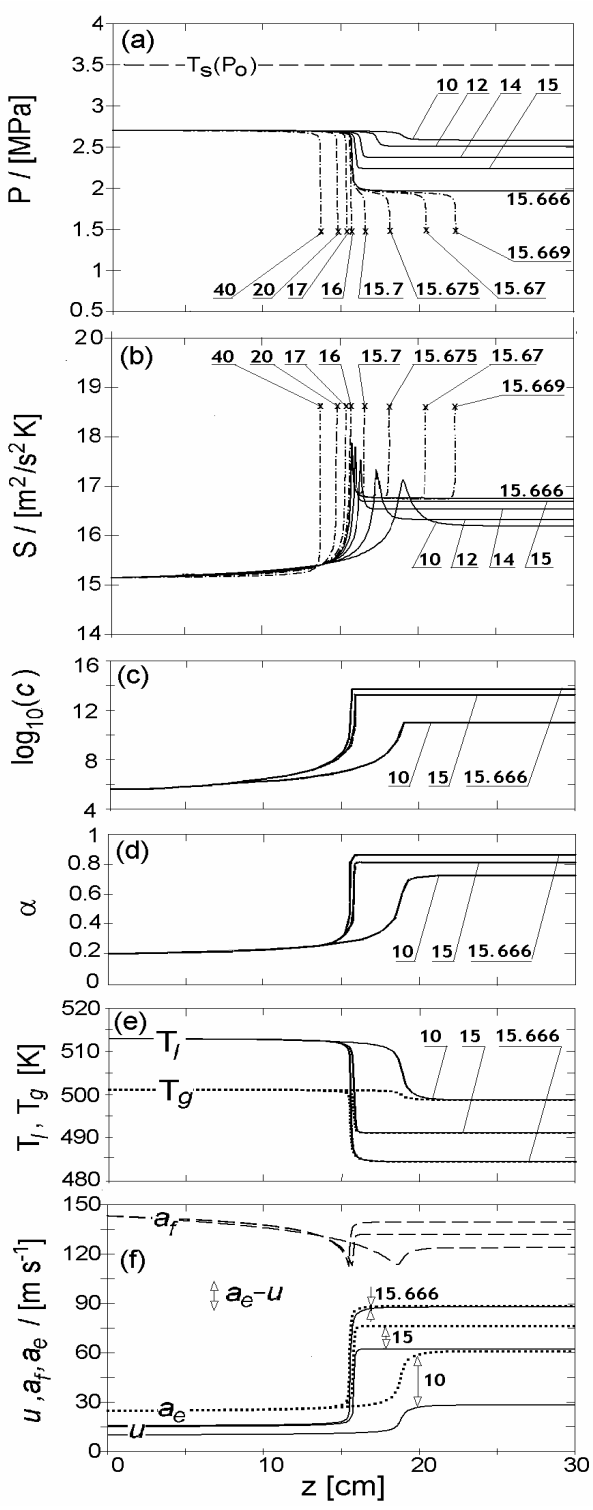

Figure 4. The structure of the boiling wave calculated using stationary model equations. The parameters at z=0 (except for the velocity of the oncoming flow) are specified being equal to that ahead of the wave front obtained in the numerical experiment using nonstationary model version. The curves correspond to different values of the flow velocity in front of the wave (shown in m s^{-1}).
(*a,b*) The distribution of the pressure and entropy along the channel for different regimes.
(*c,d,e,*f) The distribution of the other parameters for 3 wave-type regimes.

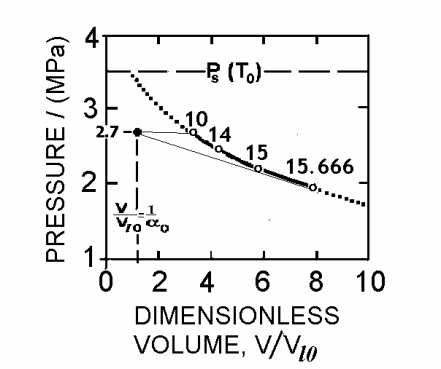

Figure 6. The Hugoniot curve with energy release, the dependence of the specific mixture volume on the pressure behind the wave. Points marked correspond to regimes with different velocities of the flow ahead of the wave's front (shown in m s^{-1}).

interphase heat exchange j approaches to zero, $d\,u/d\,z \to 0$ and the chain fragmentation is switched off. $d\,P/d\,z \to 0$ as well. As a result, 'step like' solutions (solid lines in figure 4*a*) are obtained. The regimes of this type are realized under the oncoming velocity $10\text{m/s} \le u^* \le 15.666\text{m/s}$. Entropy distribution along the channel shows entropy peak in the coordinate of the wave front. (The explanation why the entropy increase in a rarefaction wave does not contradict the 2nd law of thermodynamics may be found in the next paragraph.) The entropy value in the peak corresponds to the pressure wave amplitude, the greater the pressure fall the greater the rise in the entropy. Maximum entropy production is attained under a limit oncoming velocity value u^*=15.666 m s^{-1} when the flow accelerates up to the equilibrium sonic speed a_e (figure 4*f*). This is the regime that is realized in the calculations with the full model, as the condition $u=a_e$ ensures the 'linkage' of the wave of boiling with the waves following it.

At u^* greater than 15.666 m s^{-1}, the flow velocity increases up to the sonic one $u=a_e$ earlier than the phases come to equilibrium. The denominator in right part of (20) becomes equal to zero, parameters' gradients tend to infinity and the solutions break off (the regimes under $u^*>15.666$ m s^{-1} are shown by dashed-dotted lines in figure 4*a*). Broken-off solutions are of two types: with the pressure break-down behind the wave front section ($15.666<u^*<16$), and with the pressure tearing off at once ($u^* \ge 16$ m/s). The 'broken' entropy distributions are of two types as well (figure 4*b*).

INTEGRAL RATIOS IN FRONT OF THE BOILING SHOCK

Let us now explain why the regime with the flow velocity behind the wave equal to the equilibrium sonic speed is the one realised in a numerical experiment using a full, non-stationary, model.

The state with parameters fixed ahead of the wave front in the numerical experiment will be considered to be an initial one. For the terminal state, we claim boiling to be equilibrium: $T_l = T_S(P)$. We will link the states by the laws of the mass, impulse and energy conservation (17-19).

Let us build the dependence of the specific mixture volume on the pressure behind the wave (the Hugoniot curve).

Excluding velocities from (17-19) we obtain:

$$i_e(P,V) - i(P_0,V_0,\Delta T_{l0}) = \frac{1}{2}(V+V_0)(P-P_0) \qquad (22)$$

Where the 1st and the 2nd terms in the left-hand part are the enthalpies of an equilibrium and nonequilibrium (ahead of the wave) mixture, correspondingly; ΔT_{l0} is the liquid's overheat. Inserting

$$i(P_0,V_0,\Delta T_{l0}) - i_e(P,V) = Q_l(P_0,V_0,\Delta T_{l0}), \qquad (23)$$

we obtain the equation for an equilibrium Hugoniot curve from (22):

$$i_e(P,V) - i_e(P_0,V_0) - \frac{1}{2}(V+V_0)(P-P_0) = Q_l(P_0,V_0,\Delta T_{l0}) \qquad (24)$$

Since $\chi = \chi(P,V)$, $i_g = i_g(P)$, the only component of mixture enthalpy (9) depending on the mixture overheats is the liquid enthalpy. In correspondence with (11), (12) this dependence may be presented as follows:

$$i_{l0}(P_0,\Delta T_{l0}) = i_{le}(P_0) + c_l \Delta T_{l0}, \quad i_{le}(P_0) = i_{ls}(T_s(P_0)).$$

Having substituted this equation for i_{l0} into (9) we obtain the expression for the inequilibrium mixture enthalpy in the form:

$$i(P_0,V_0,\Delta T_{l0}) = i_e(P_0,V_0) + (1-\chi_0)c_l \Delta T_{l0}. \qquad (25)$$

The second term in the right-hand part of this expression is the energy of an initial liquids' overheat. Comparing (23) with (25) we see that

$$Q_l(P_0,V_0,\Delta T_{l0}) = (1-\chi_0)h\Delta T_{l0}.$$

That is Q_l is positive. For waves with $Q_l > 0$, it has been shown that the entropy increases across the wave front for both compression and rarefaction waves, in contrast to waves with $Q_l \le 0$. Thus the entropy increase in a rarefaction wave (figure 4*a,b*) does not contradict the second law of thermodynamics.

The equation for the equilibrium sonic speed may be obtained by differentiating of the equation for the equilibrium mixture state:

$$\frac{1}{a_e^2} = \left(\frac{\partial\rho}{\partial P}\right)\Bigg|_{S=\text{const}} =$$

$$= \frac{\rho^2}{\rho_l^2 a_l^2} + \rho\left[\left(1-\frac{\rho}{\rho_l}\right)\frac{1}{\varphi}\left(\frac{\partial^2 T}{\partial P^2}\right)_S - \frac{\rho\varphi}{\rho_l T}\left(\rho_l\left(\frac{\partial i_l}{\partial P}\right)_S - 1\right)\right].$$

Under the analysis usually carried for Hugoniot curves with heat release [9], it has been shown that a maximal flow rate through the shock wave front is attained when the flow rate behind the wave front is equal to the equilibrium sonic speed since the flow is equilibrium behind the wave.

Among the wave-type stationary regimes there is one with the flow speed equal to the equilibrium sonic speed behind the wave front (under u^*=15.666 m/s in figure 4*f*), this regime being just the one obtained in a numerical experiment using full, nonstationary, boiling flow model equations. The realization of the regime with a maximum mass flow rate may be regarded as the implementation of Jouguet's hypothesis set up for combustion waves for the waves of boiling.

CONCLUSIONS

The phenomenon of shock boiling under a high-pressure-vessel decompression has been simulated using boiling flow model which considers phases to be non-equilibrium in temperatures and velocities.

The shock wave structure investigation using stationary equations in the moving frame linked with the wave's front has shown that a quick boiling mixture transformation into an equilibrium state is caused by a chain bubble fragmentation which led to a fast loss of liquid's excess heat by means of a sharp increase in the interfacial area.

For the stationary model system solution, all the parameters ahead of the wave front but the velocity of the oncoming flow were taken from the numerical experiment using a full, non-stationary, system of model equations. There were obtained a set of wave-type regimes each characterizing by a definite meaning of the entropy increase in a shock. It occurred that, in a numerical experiment on depressurization that was in good agreement with the physical one there realized the regime with the maximum entropy production.

ACKNOWLEDGMENT

The work was supported by the Russian Foundation for Basic Research (grant no. 12-08-162a).

NOMENCLATURE

Symbol	Quantity	SI Unit
a	Speed of sound	m s^{-1}
A	Approximation parameter	m^2 s^{-2}
c	Bubble number per unit mixture mass	kg^{-1}
B	specific heat of the liquid on saturation curve	m^2 s^{-2} K^{-1}
C_{vm}	Virtual mass coefficient	dimensionless
C_μ	Interfacial drag coefficient	dimensionless
D	Constant in the approximation dependence for liquid enthalpy on a saturation curve	K
G	Mass flow rate	kg m^{-2} s^{-1}
h	Specific heat capacity of the liquid	m^2 s^{-2} K^{-1}
i	Specific enthalpy	m^2 s^{-2}
$I(\lambda)$	Decrement of a wave	s^{-1}
j	Intensity of liquid evaporation into a bubble	kg s^{-1}
Ja	Jacob number	dimensionless
k	Constant in the equation for the liquid state	m^3 kg^{-1}
K	Constant number symbol	dimensionless
l	Specific heat of liquid vaporization	m^2 s^{-2}
n	Bubble number per unit mixture volume	m^{-3}
Nu	Nusselt number	dimensionless
P	Pressure	kg m^{-1} s^{-2}
r	Bubble radius	m
Re	Bubble Reynolds number	dimensionless
S	Entropy	m^2 s^{-2} K^{-1}
t	time	s
T	Temperature	K
u	Velocity	m s^{-1}
V	Specific volume	m^3 kg^{-1}
We	Weber number	dimensionless
x	Coordinate	m
z	Coordinate in a moving frame	m
α	Volumetric vapour fraction	dimensionless
β	Coefficient of the liquid compressibility	kg m^{-2} s^{-1}
χ	Mass vapour fraction	dimensionless
γ	Coefficient of the thermal conductivity for the liquid	kg m s^{-3} K
λ	Wavelength	m
μ	Dynamic viscosity coefficient	kg m^{-1} s^{-1}
ρ	Mixture density	kg m^{-3}
σ	Coefficient of the surface tension	kg s^{-2}
τ	Fragmentation time	s
ξ	Perturbation amplitude	m
ψ	Intensity of bubble fragmentation	kg^{-1} s^{-1}
e	Refers to the 'equilibrium' mixture characteristic	
f	Refers to the 'frozen' mixture characteristic	
g	Refers to the vapour phase	
l	Refers to the liquid phase	
s	Refers to a saturation condition	
0	Refers to an initial condition	
$*$	Refers to a critical condition	

REFERENCES

[1] A.R. Edwards and T.P. O'Brien, Studies on phenomena connected with the depressurization of water reactors, *J. Brit. Nucl. Engng Soc.*, vol. 9, pp. 125–135, 1970.

[2] O.A. Isaev, Luquid boiling under a fast pressure fall in an adiabatic unsteady stream, Ph.D. thesis, Sverdlovsk, 1980 (in Russian).

[3] W.S. Jr. Winters and H.Jr. Merte, Experiments and nonequilibrium analysis of pipe blowdown, *Nucl. Sci. Engng.*, vol 69 (3), pp. 411-429, 1979.

[4] A.I. Ivandaev and A.A. Gubaidullin, The investigation of an unsteady efflux of boiling liquid in a thermodynamically equilibrium approximation, *Teplofiz. Vys. Temp.*, vol 16 (3), pp. 556-562, 1978 (in Russian).

[5] G. Lamb, Hydrodynamics, Cambridge University Press, Cambridge, 1957.

[6] R.I. Nigmatulin and K.I. Soplenkov, The study of an unsteady efflux of boiling liquid from channels in the thermodynamically non-equilibrium approximation, *Teplofiz. Vys. Temp.*, vol. 18 (1), pp. 118-131, 1980 (in Russian).

[7] L.E. Scriven, On the dynamics of phase growth, *Chem Engng Sci.*, vol. 10, pp. 1-13.

[8] O.E. Ivashnyov and K.I. Soplenkov, A model involving break-up to explain pecularities of boiling liquid efflux process, *Intl J. Multiphase Flow*, vol. 18 (5), pp. 727-738, 1992.

[9] N.N. Smirnov and I.N. Zverev, Heterogeneous burning, Moscow University Press, Moscow, 1992 (in Russian).